

## Research Article

# Manipulating the Laser-Driven Proton Bunch with Plasma Wakefield

Chao Jin <sup>1,2</sup> Xiao-ying Zhao <sup>1,2</sup> Han-jie Cai <sup>1,2</sup> Xin Qi <sup>1,2</sup> Zhi-jun Wang <sup>1,2</sup>  
and Yuan He <sup>1,2</sup>

<sup>1</sup>*Institute of Modern Physics, Chinese Academy of Science, Lanzhou 730000, China*

<sup>2</sup>*School of Nuclear Science and Technology, University of Chinese Academy of Science, Beijing 100049, China*

Correspondence should be addressed to Xin Qi; [qixin2002@impcas.ac.cn](mailto:qixin2002@impcas.ac.cn)

Received 6 June 2022; Revised 24 November 2022; Accepted 9 December 2022; Published 19 December 2022

Academic Editor: Yongtao Zhao

Copyright © 2022 Chao Jin et al. This is an open access article distributed under the Creative Commons Attribution License, which permits unrestricted use, distribution, and reproduction in any medium, provided the original work is properly cited.

With the advantages of short duration and extreme brightness, laser proton accelerators (LPAs) show great potential in many fields for industrial, medical, and research applications. However, the quality of current laser-driven proton beams, such as the broad energy spread and large divergence angle, is still a challenge. We use numerical simulations to study the propagation of such proton bunches in the plasma. Results show the bunch will excite the wakefield and modulate itself. Although a small number of particles at the head of the bunch cannot be manipulated by the wakefield, the total energy spread is reduced. Moreover, while reducing the longitudinal energy spread, the wakefield will also pinch the beam in the transverse direction. The space charge effect of the bunch is completely offset by the wakefield, and the transverse momentum of the bunch decreases as the bunch transports in the plasma. For laser-driven ion beams, our study provides a novel idea about the optimization of these beams.

## 1. Introduction

During the last decade, plasma-based particle accelerators driven by high-intensity ultrashort laser pulses [1–3] or particle beams have shown great promise, primarily because of the extremely large accelerating electric fields that they can support, about a thousand times greater than conventional accelerators, enabling the realization of laboratory-scale applications ranging from high-energy physics to ultrabright light sources.

For proton accelerations, target normal sheath acceleration (TNSA) [4, 5], radiation pressure acceleration (RPA) [6, 7] and breakout afterburner (BOA) [8] are the most widely employed mechanisms. Despite the relatively low energy transfer efficiency, TNSA is considered the most robust and stable mechanism, where the ions (especially protons) from the surface contamination layer are accelerated by the charge separation sheath field. Since several experiments have demonstrated large accelerations, the resulting beam quality is still far from state-of-the-art conventional accelerators: due to the rapid diffusion of the

electron layer, Coulomb explosion, and multiple instabilities, TNSA ion beams are characterized by an exponentially decaying energy spectrum and a large divergence angle [9]. Thus, one of the main goals is to control the energy divergence and shape the beam.

Various beamlines have been proposed at several institutes, for instance, the light beam line at GSI Helmholtz Center [10, 11], the ELIMED beamline installed in Prague [12] and the CLAPA platform at Peking University [13, 14]. These beamlines are designed to realize the propagation of high current and dense ion beams with low energy spread and with reliability, availability, maintainability, and inspectability.

Compared with these beamlines, which are composed of conventional accelerator elements such as permanent magnet quadrupole lenses, solenoid magnets, and laser-triggered microlenses, recent experiments show that when electron beams propagate in a plasma element, the plasma wakefield will tune the longitudinal phase space of the electron beams and reduce the energy spread. For example, FLASHForward plasma-accelerator facility at DESY [15]

showed that in beam-driven plasma acceleration, if an electron bunch acts as a driver, while an ultrashort witness bunch with positive energy chirp follows behind, the longitudinal phase space of the witness bunch will be rotated during acceleration, resulting in an ultralow energy spread that is even lower than the spread at the plasma entrance. Another experiment at the SPARC LAB test facility [16] demonstrated that high efficiency and low energy spread can be achieved simultaneously by strong beam loading of plasma wakefields when accelerating bunches with carefully tailored current profiles. In both experiments above, there are two bunches: the driven bunch creates wakefields, while the energy spread of the witness bunch is reduced in these wakefields. Another experiment shows that even for a single electron bunch with negative chirp passing through plasmas, its wakefields will manipulate the longitudinal phase space (LPS) along the beam itself, and reduce the total energy spread [17, 18].

These experiments mainly concern about electron bunches. For proton accelerations, the proton beams have the typical exponentially decaying spectrum and positive energy chirp. In this paper, we employ the two-dimensional particle-in-cell (PIC) algorithm [19, 20] to study the propagation of such beams in plasmas. The effect of plasma wakefield on longitudinal energy spread, as well as the transverse compression of a single proton bunch are investigated. The main contents of this paper are as follows: Section 2 introduces the physical model used in our simulations. In Section 3, the simulation results are presented and discussed. Finally, conclusions are made in Section 4.

## 2. Materials and Methods

The physical model is shown in Figure 1. The proton bunch propagates from left to right in the hydrogen plasma channel. Assuming the plasma is collisionless, nonpolarized, and stable.

Normally, the proton beam produced by LPA has the characteristics of exponential decay energy distribution. The particle number spectrum  $dN/dE$  follows the formula:  $dN/dE = (N_0/\sqrt{2Ek_B T})e^{-\sqrt{2E/k_B T}}$  [5]. The bunch needs to be selected in advance by the sector magnet and a slit: when the beam with broad energy spread passing the sector magnet ( $x$  (horizontal) direction), protons with different energies are dispersed along the  $x$  axis. Then, a slit is used to choose the bunch with expected energy. In Figure 2(a), the blue line is the energy spectrum of the beam generated by the LPA and the red line is the one we chose to use as the initial bunch for simulations. The initial bunch has an exponentially decaying energy spectrum, and the energy of the particles in the bunch is 44.75 MeV to 45.25 MeV. In addition, since the duration of the bunch generated by the laser accelerator is usually very short (a few ps, and the longitudinal positions of protons with different energies are basically the same), the longitudinal phase space of the bunch after propagating a given distance depends mainly on the energy distribution. The longitudinal positions of 44.75 MeV protons and 45.25 MeV protons are basically the same when they are generated by the laser accelerator. After

propagating 60.3 ns (propagation of about 5.4 m), they will be separated by 28 mm (the length of the beam used in the simulation) due to different velocities. The relationship between energy and velocity is not linear, but when the proton is between 44.75 MeV and 45.25 MeV, the relationship between energy and velocity is very close to linear, so the longitudinal phase space of the initial bunch is shown in Figure 2(b). Due to the space charge effect, disturbance is added to the initial bunch. The initial bunch used in the simulation is shown in Figure 2(c).

The wavelength of the wakefield is  $\lambda_w = (2\pi v_b/\omega_e) = 31.5\text{mm}$ , where  $\omega_e = \sqrt{(N_{e0}e^2/\epsilon_0 m_e)}$ . We choose the bunch length  $L_B = 28\text{mm}$ , which is slightly smaller than the wakefield wavelength, and the bunch RMS radius  $= 0.36\text{mm}$ . The bunch is initially a Gaussian distribution (Figure 3(a)). The transverse phase space of the initial bunch is shown in Figure 3(b) and  $y'$  size (Rms)  $= 0.94\text{mrad}$ . A laser accelerator produces a bunch with particle numbers between  $10^8$  and  $10^{12}$  per MeV (the number of particles decreases exponentially with energy growth) [21, 22]. To make the modulation of the beam in the plasma more obvious, we chose a higher current intensity than the experiment. The initial beam used in the simulation contains  $1.92 \times 10^{12}$  protons, and the bunch density is  $Nb_0 = 9.52 \times 10^{16}\text{m}^{-3}$ . We select the plasma density  $N_{e0}$  according to the bunch density,  $N_{e0} = 1 \times 10^{17}\text{m}^{-3}$ . The plasma density distribution is shown in Figure 3(c), plasma temperature  $T_{e0} = T_{i0} = 1\text{eV}$ .

The software VORPAL [23] code is used to simulate the propagation of proton bunch in the plasma. All simulations are performed by a 2D3V PIC algorithm. The length of the simulation area  $L_z$  is 0.338 m, while the width  $L_y$  0.024 m. 7200 grids in the  $z$  direction and 512 grids in the  $y$  direction are used. Moreover, open boundary condition is employed in both  $z$  and  $y$  direction. Spatial step  $dz = dy = 2 * \lambda_e = 4.7 * 10^{-5}\text{m}$ , where  $\lambda_e$  is Debye length of the plasma. The time step  $dt = 8.1475 \times 10^{-14}\text{s}$ .

## 3. Results and Discussion

Figure 4 is the time evolution of the LPS as the proton bunch passes through the plasma. Figures 4(a)–4(d) are results when the bunch propagates in the plasma at distance of 0, 7.2, 14.4, and 21.6 cm, respectively. The solid line is the longitudinal electric field on the axis at the bunch position. Figures 4(e)–4(h) is the corresponding electron distribution in plasma. When passing through the plasma, the protons at the head of the bunch will disturb the electron distribution in the plasma and create a wakefield. This wakefield will affect the subsequent protons in the bunch. For a bunch with the positive energy chirper, the wakefield reduces the energy spread due to that the first half of the protons in the bunch lose their energy and create the wakefield, while the latter half of the protons gain energy from it. Thus, the total energy spread of the bunch is reduced. As shown in Figures 4(c) and 4(d), protons at the tail of the bunch are in a longitudinal accelerating electric field, while protons are in front under the effect of the deceleration field. It is noted that although the wakefield can modulate the energy spread, there is still a

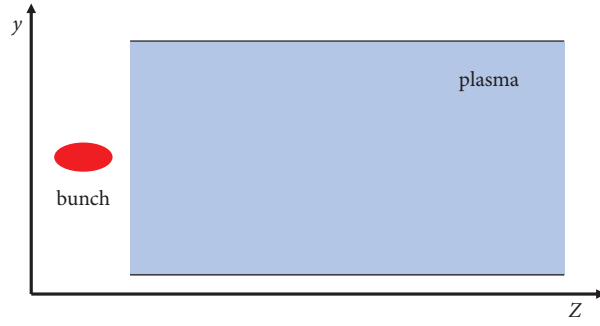


FIGURE 1: Two-dimensional simulation model: proton bunch propagates in the plasma.

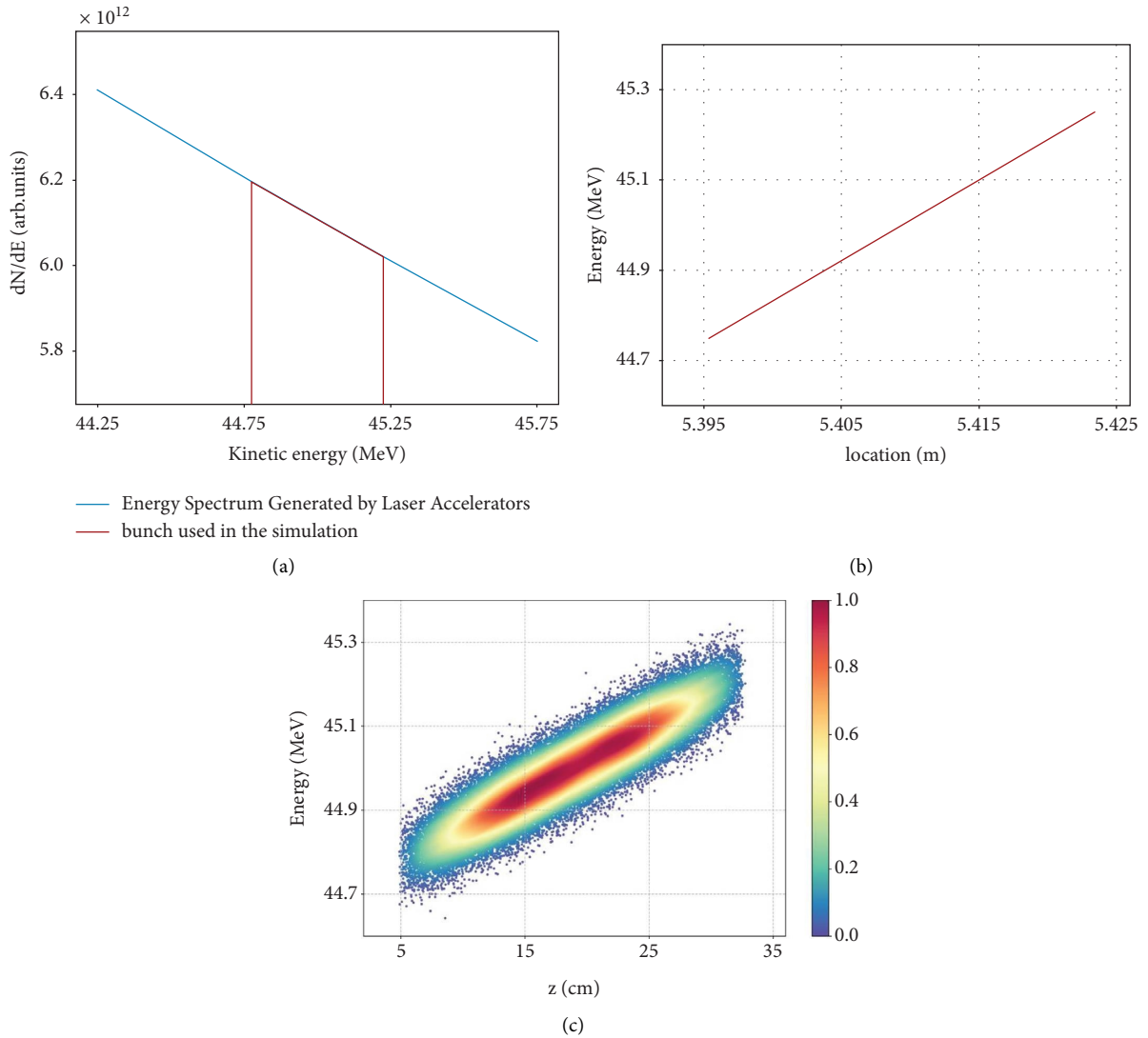


FIGURE 2: (a) The blue line is the energy spectrum of the bunch generated by the laser accelerator. The red line is the energy spectrum of the bunch after passing through the sector magnet and the slit, using this bunch as the initial bunch for the simulation. (b) Distribution of longitudinal positions of protons with different energies produced by laser accelerator after 60.3 ns of transmission. (c) Longitudinal phase space of initial bunch.

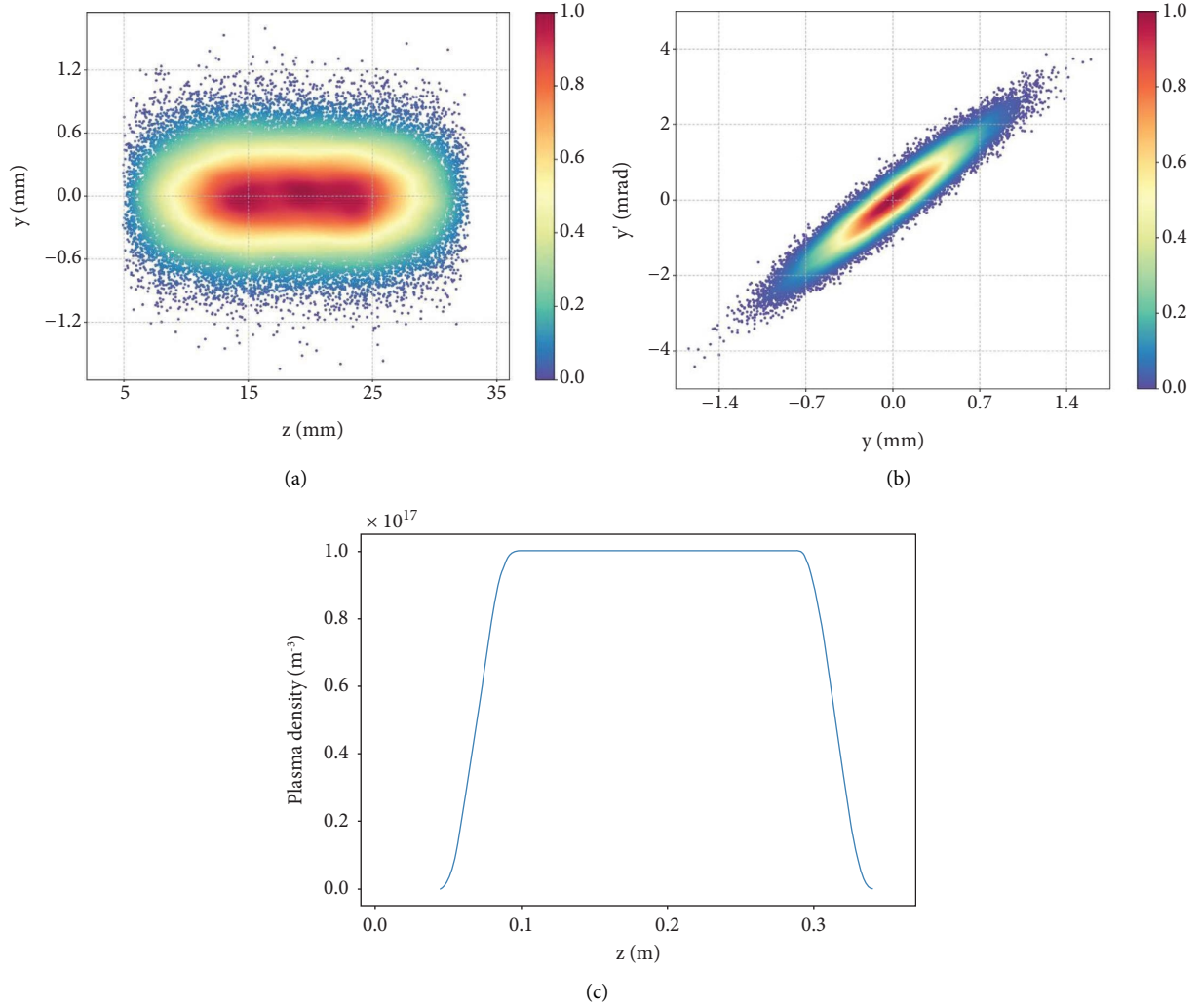


FIGURE 3: (a) Distribution of the initial bunch, (b) transverse phase space of the initial bunch, and (c) the distribution of plasma density in the longitudinal direction.

small accelerating electric field at the very head of the bunch. This accelerating electric field is caused by the space charge effect of the bunch: the wakefield only exists behind the bunch; thus, protons at the very head of the bunch cannot be affected. Therefore, these proton's energies will continue to diverge by Coulomb's repulsive force.

Figure 5 is the time evolution of the energy spectrum of the bunch. Figure 5(a) is the initial energy spectrum of the bunch with exponentially decaying energy distribution (The exponential decay of the particle number is not obvious due to the small energy spread). The initial energy spread is 0.5 MeV (44.75 MeV to 45.25 MeV). As the bunch passes through the plasma, although few protons at the very head of the bunch cannot be modulated, the energy of the rest protons begins to concentrate. When the bunch passes through the plasma, more than 50% of the proton energies are in the range from 44.85 MeV to 44.95 MeV. That is to say, the energy spread of half protons is concentrated to 0.2% by the plasma modulation, as shown in Figure 5(d).

The control of the transverse divergence of the bunch is another challenge. Figures 6(a) and 6(b) are the distribution and the transverse phase space of the bunch when the bunch passes through the plasma, while Figures 6(c) and 6(d) are the comparison of the bunch passing through a vacuum pipe at the same distance. Compared with these in a vacuum, the transverse distributions of the bunch in plasma are reduced for both position and momentum. In particular, the momentum distribution decreases significantly. This is due to that the protons are heavy. When passing through a plasma channel of only 21.6 cm, the wakefield significantly changes its momentum, but it has not significantly affected its position distribution yet.

Another phenomenon in Figures 6(a) and 6(b) is that the transverse compression at the rear of the bunch is more obvious. To further investigate it, the corresponding longitudinal electric field  $E_z$ , transverse electric field  $E_y$ , as well as the magnetic field  $B_x$  are shown in Figures 7(a)–7(c), separately. Figure 7(a) is the distribution of the longitudinal

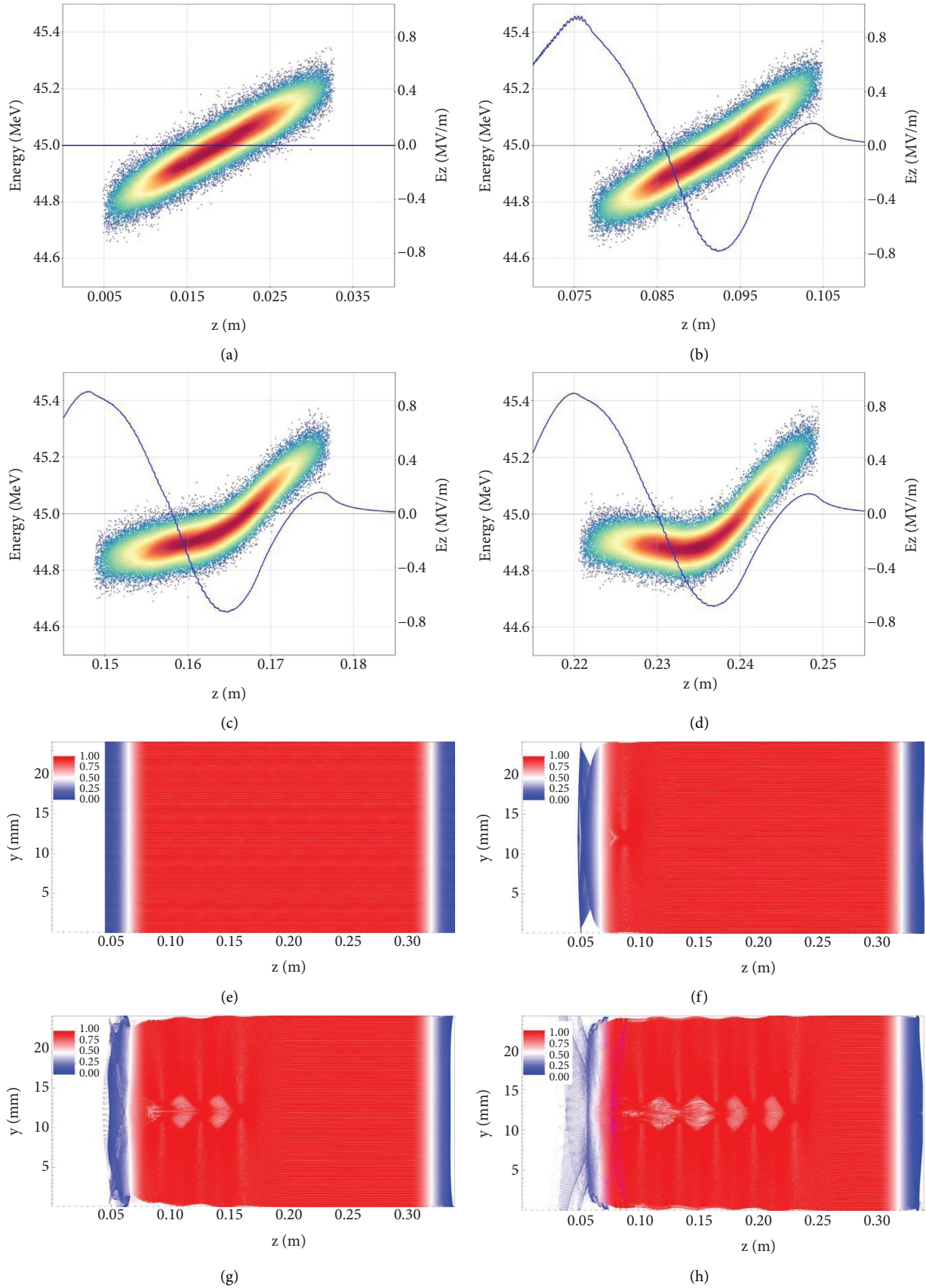


FIGURE 4: (a–d) Beam longitudinal phase space (dot) and longitudinal plasma wakefield  $E_x$  (blue line). (e–h) The corresponding electron distribution in plasma. (a) Initial bunch energy distribution. (e) Initial electron distribution in plasma. (b, f) Propagation distance of bunch  $s = 7.2$  cm. (c, g) Propagation distance of bunch  $s = 14.4$  cm. (d, h) Propagation distance of bunch  $s = 21.6$  cm.

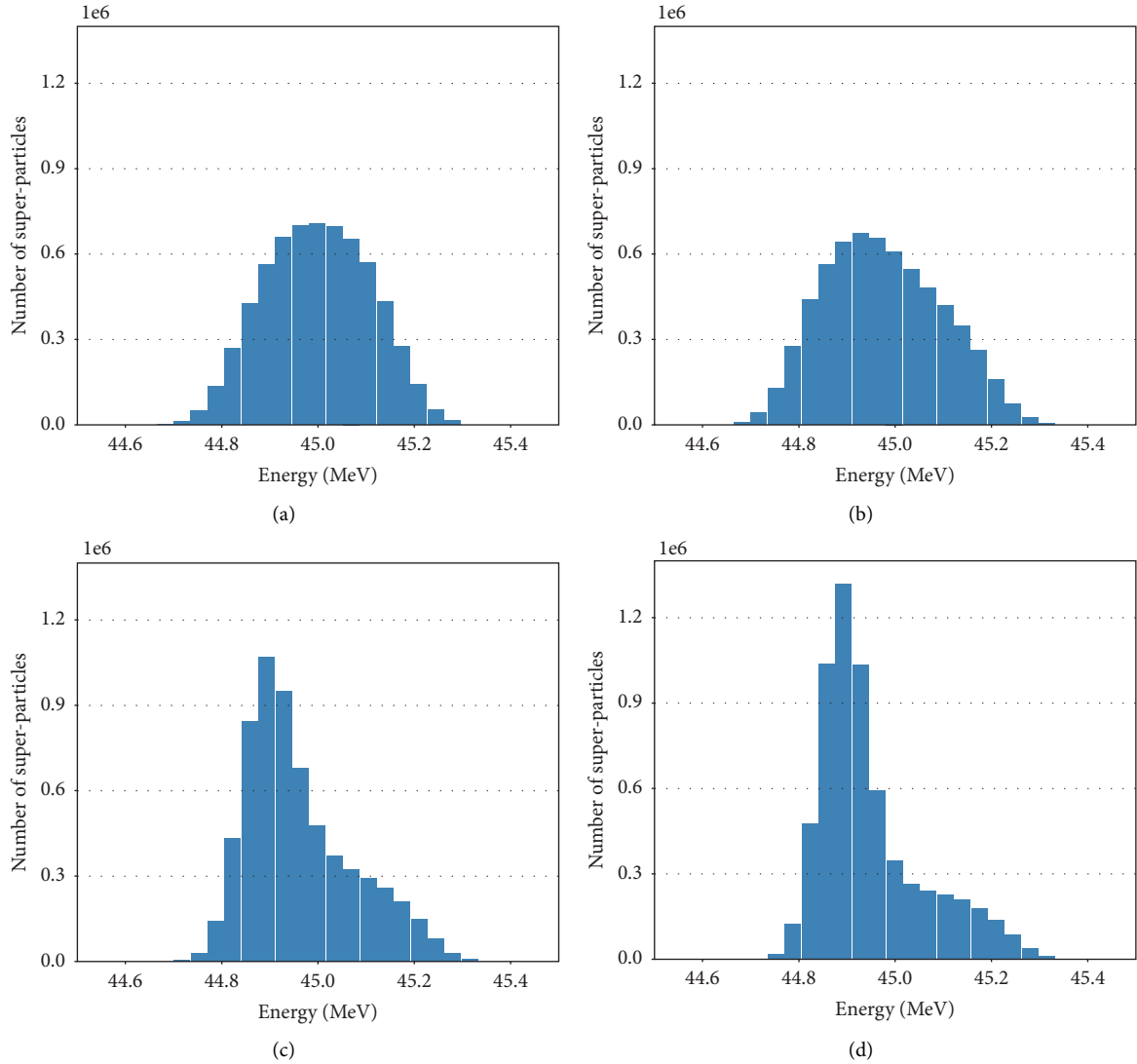


FIGURE 5: Energy spectrum of the bunch. (a) Initial bunch energy spectrum. Propagation distance  $s=0$  cm, (b) propagation distance  $s=7.2$  cm, (c) propagation distance  $s=14.4$  cm, and (d) propagation distance  $s=21.6$  cm.

electric field. As discussed above, it is periodic and goes with the bunch. The head of the bunch is in the deceleration field, while the rest is in the acceleration field. Figure 7(b) is the distribution of the transverse electric field  $E_y$ . The transverse defocuses and the focus regions alternately appear. The head of the bunch is in the defocus region while the rear of the bunch is in the focus region. Moreover, the total bunch is surrounded by the magnetic field, as shown in Figure 7(c). For protons in the first half of the bunch, although they are in the transversely divergent electric field, they are pinched by the magnetic field at the same time. Thus, the plasma still limits its transverse divergence. The rear protons are in the transverse focusing electric field and pinched magnetic field

at the same time, so the transverse compression effect is more obvious.

The envelop curves of the transverse position and momentum versus the longitudinal position of the bunch are shown in Figure 8. The blue lines represent the result of bunch propagation in plasma, while the red lines are the result in a vacuum. Plasma can reduce the transverse divergence of the bunch. It is noted that the bunch stays in the plasma for only 2.4 ns (propagation distance 21.6 cm), therefore, the plasma cannot compress the transverse size of the bunch in such a short time. However, the wakefield of the plasma has significantly changed the transverse momentum of the bunch. As shown in Figure 8(b), the final transverse

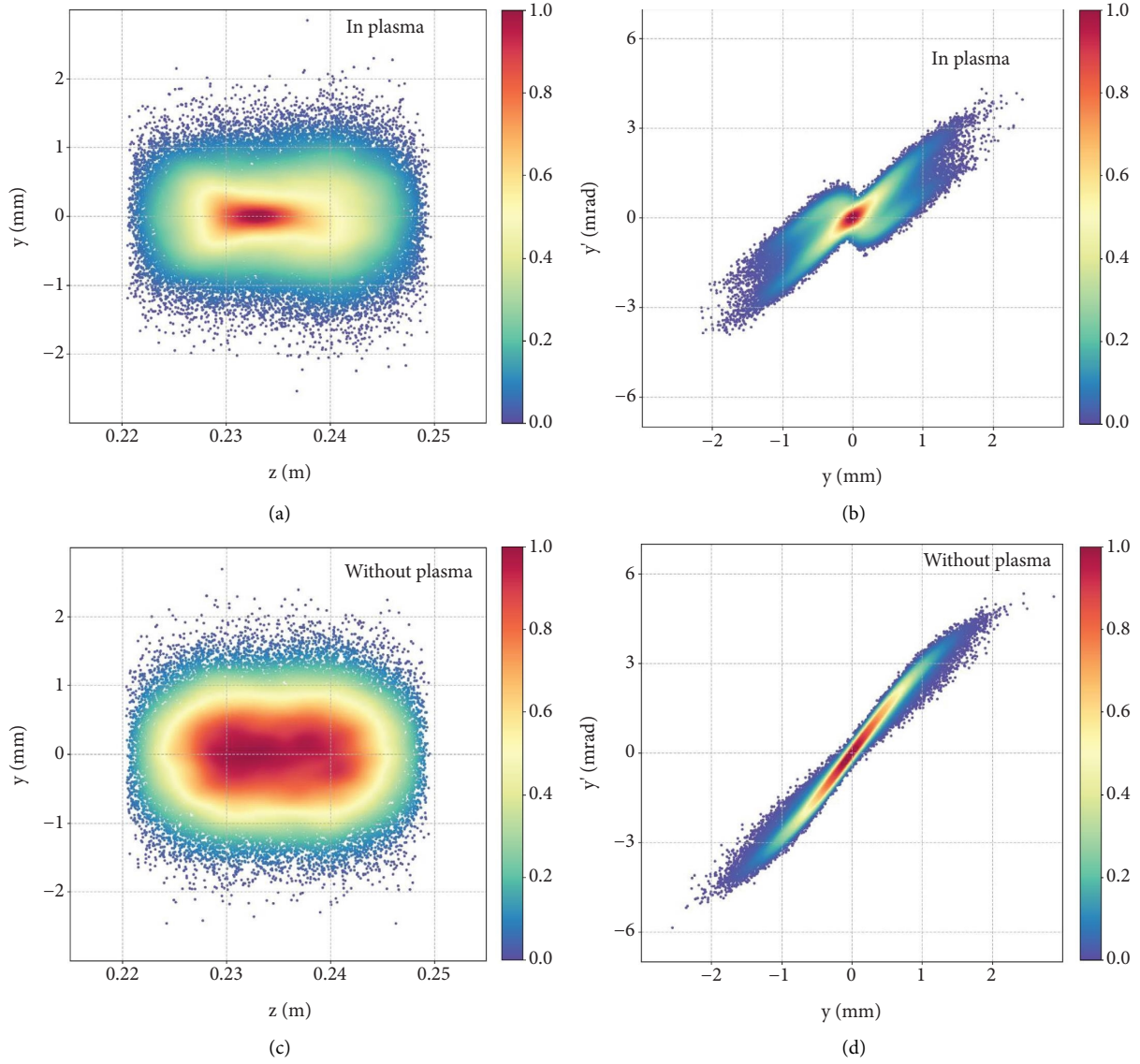


FIGURE 6: (a, b) The distribution and the transverse phase space of the bunch after the bunch transmits 21.6 cm in the plasma. (c, d) The distribution and the transverse phase space of the bunch after the bunch transmits 21.6 cm in the vacuum.

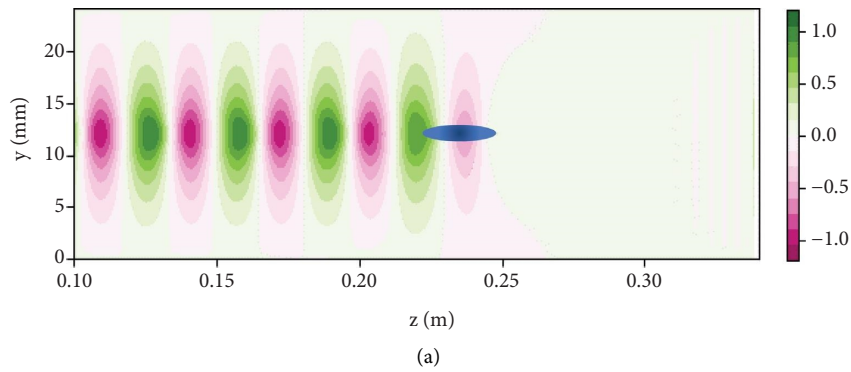


FIGURE 7: Continued.

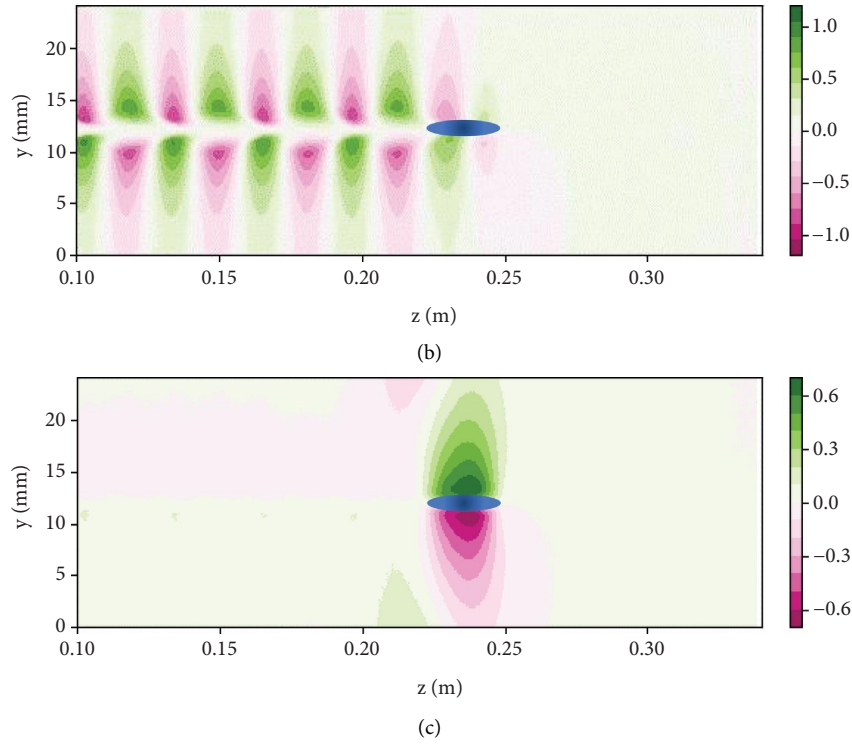


FIGURE 7: The electric and magnetic field ( $E_x$ ,  $E_y$ , and  $B_z$ ) in the wakefield region induced by the proton bunch traveling through the plasmas and propagation distance  $s = 21.6$  cm. The blue ellipse in the figure represents the bunch. (a) Longitudinal electric field distribution in plasma (unit is MV/m), (b) transverse electric field distribution in plasma (unit is MV/m), and (c) magnetic field in the direction which perpendicular to the propagation plane (unit is mT).

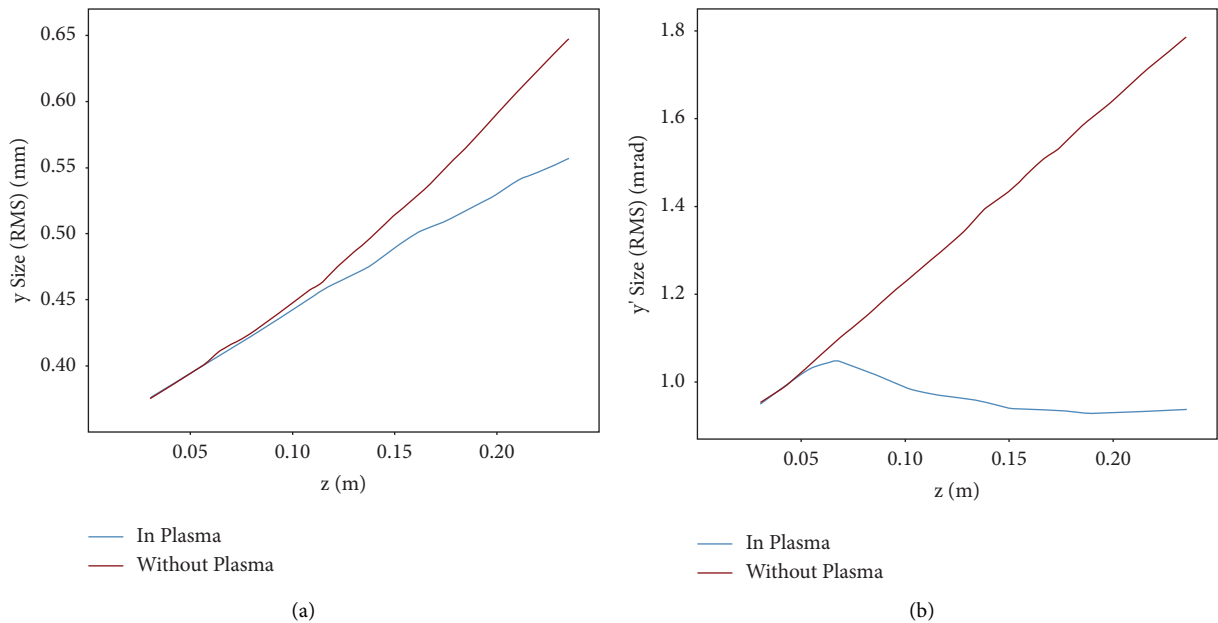


FIGURE 8: Variation of the transverse size of the bunch when propagating in plasma.

momentum of the bunch is lower than that before entering the plasma, which means that the wakefield not only completely neutralizes Coulomb's repulsion force but also starts to pinch the bunch.

#### 4. Conclusions

In this paper, we use PIC simulations to study the propagation of a laser-driven proton bunch in the plasma. Our results show



that the laser-driven proton beams, of which are characterized by large energy spread and divergence angles, can be modulated by the plasma wakefield. The bunch will excite the wakefield and modulate itself. Although a small number of particles at the head of the bunch cannot be modulated by the wakefield, the total energy spread is concentrated. Especially, for a proton bunch with energies between 44.75 MeV and 45.25 MeV, the energy of more than half of the protons is concentrated between 44.85 and 44.95 by plasma modulation. Moreover, while reducing the longitudinal energy spread, the wakefield will also pinch the beam in the transverse direction. The space charge effect of the bunch is completely offset by the wakefield, and the transverse momentum of the bunch decreases as the bunch transports in the plasma. For laser-driven proton beams, the bunches are characterized by large energy spread and divergence angles, which is difficult to optimize with traditional accelerator elements. The paper provides a novel idea for solving this problem.

### Data Availability

The source code and data that support the findings of this study are available upon request from the corresponding authors.

### Conflicts of Interest

The authors declare that they have no conflicts of interest.

### Acknowledgments

This work was supported by the National Natural Science Foundation of China (Grant nos. 11775282 and 11805253), the Youth Innovation Promotion Association CAS (Grant no. 2018452), and Large Research Infrastructures “China Initiative Accelerator Driven System” (Grant no. 2017-000052-75-01-000590).

### References

- [1] J. Ding, D. Schumacher, D. Jahn, A. Blazevic, and M. Roth, “Simulation studies on generation, handling and transport of laser-accelerated carbon ions,” *Nuclear Instruments and Methods in Physics Research Section A: Accelerators, Spectrometers, Detectors and Associated Equipment*, vol. 909, 2018.
- [2] I. J. Kim, K. H. Pae, I. W. Choi et al., “Radiation pressure acceleration of protons to 93 MeV with circularly polarized petawatt laser pulses,” *Physics of Plasmas*, vol. 23, no. 7, Article ID 070701, 2016.
- [3] A. Higginson, R. J. Gray, M. King et al., “Near-100 MeV protons via a laser-driven transparency-enhanced hybrid acceleration scheme,” *Nature Communications*, vol. 9, no. 1, p. 724, 2018.
- [4] B. M. Hegelich, B. J. Albright, J. Cobble et al., “Laser acceleration of quasi-monoenergetic MeV ion beams,” *Nature*, vol. 439, no. 7075, pp. 441–444, 2006.
- [5] J. Fuchs, P. Antici, E. D’Humières et al., “Laser-driven proton scaling laws and new paths towards energy increase,” *Nature Physics*, vol. 2, no. 1, pp. 48–54, 2006.
- [6] T. Esirkepov, M. Borghesi, S. V. Bulanov, G. Mourou, and T. Tajima, “Highly efficient relativistic-ion generation in the laser-piston regime,” *Physical Review Letters*, vol. 92, no. 17, Article ID 175003, 2004.
- [7] A. Macchi, F. Cattani, T. V. Liseykina, and F. Cornolti, “Laser acceleration of ion bunches at the front surface of overdense plasmas,” *Physical Review Letters*, vol. 94, no. 16, Article ID 165003, 2005.
- [8] L. Yin, B. J. Albright, K. J. Bowers, D. Jung, J. C. Fernández, and B. M. Hegelich, “Three-dimensional dynamics of breakout afterburner ion acceleration using high-contrast short-pulse laser and nanoscale targets,” *Physical Review Letters*, vol. 107, no. 4, Article ID 045003, 2011.
- [9] U. Linz and J. Alonso, “Laser-driven ion accelerators for tumor therapy revisited,” *Physical Review Accelerators and Beams*, vol. 19, no. 12, p. 124802, 2016.
- [10] D. Jahn, D. Schumacher, C. Brabetz et al., “First application studies at the laser-driven LIGHT beamline: improving proton beam homogeneity and imaging of a solid target,” *Nuclear Instruments and Methods in Physics Research Section A: Accelerators, Spectrometers, Detectors and Associated Equipment*, vol. 909, pp. 173–176, 2018.
- [11] S. Busold, D. Schumacher, C. Brabetz et al., “Towards highest peak intensities for ultra-short MeV-range ion bunches,” *Scientific Reports*, vol. 5, no. 1, Article ID 12459, 2015.
- [12] F. Romano, F. Schillaci, G. Cirrone et al., “The ELIMED transport and dosimetry beamline for laser-driven ion beams,” *Nuclear Instruments and Methods in Physics Research Section A Accelerators Spectrometers Detectors and Associated Equipment*, vol. 829, pp. 153–158, 2016.
- [13] J. Zhu, M. Wu, K. Zhu et al., “Demonstration of tailored energy deposition in a laser proton accelerator,” *Physical Review Accelerators and Beams*, vol. 23, no. 12, Article ID 121304, 2020.
- [14] J. G. Zhu, M. Wu, Q. Liao et al., “Experimental demonstration of a laser proton accelerator with accurate beam control through image-relaying transport,” *Physical Review Accelerators and Beams*, vol. 22, no. 6, Article ID 061302, 2019.
- [15] R. Pompili, D. Alesini, M. P. Anania et al., “Energy spread minimization in a beam-driven plasma wakefield accelerator,” *Nature Physics*, vol. 17, no. 4, pp. 499–503, 2021.
- [16] C. Lindström, J. M. Garland, S. Schröder et al., “Energy-spread preservation and high efficiency in a plasma-wakefield accelerator,” *Physical Review Letters*, vol. 126, no. 1, p. 014801, 2021.
- [17] Y. Wu, J. Hua, Z. Zhou et al., “Phase space dynamics of a plasma wakefield dechirper for energy spread reduction,” *Physical review letters*, vol. 122, 2019.
- [18] V. Shpakov, M. P. Anania, M. Bellaveglia et al., “Longitudinal phase-space manipulation with beam-driven plasma wakefields,” *Physical Review Letters*, vol. 122, no. 11, p. 114801, 2019.
- [19] L. Y. Zhang, X. Y. Zhao, X. Qi, W. S. Duan, and L. Yang, “Particle-in-cell simulations of the long proton beam focusing in background plasmas,” *Laser and Particle Beams*, vol. 34, no. 2, pp. 299–305, 2016.
- [20] N. Kumar, A. Pukhov, and K. Lotov, “Self-modulation instability of a long proton bunch in plasmas,” *Physical Review Letters*, vol. 104, no. 25, Article ID 255003, 2010.
- [21] F. Wagner, O. Deppert, C. Brabetz et al., “Maximum proton energy above 85 MeV from the relativistic interaction of laser pulses with micrometer ThickCH<sub>2</sub>Targets,” *Physical Review Letters*, vol. 116, no. 20, Article ID 205002, 2016.
- [22] K. Harres, I. Alber, A. Tauschwitz et al., “Beam collimation and transport of quasinneutral laser-accelerated protons by a solenoid field,” *Physics of Plasmas*, vol. 17, no. 2, Article ID 023107, 2010.
- [23] C. Nieter and J. R. Cary, “VORPAL: a versatile plasma simulation code,” *Journal of Computational Physics*, vol. 196, no. 2, pp. 448–473, 2004.